

The Onset of Electrical Breakdown in Dust Layers:

II. Effective Dielectric Constant and Local Field Enhancement

Ronald P. Young and James L. DuBard

Southern Research Institute
Birmingham, Alabama

Leslie E. Sparks

U.S. Environmental Protection Agency
Research Triangle Park, North Carolina

Part I of this work has shown that electrical breakdown in dust layers obeys Paschen's Law, but occurs at applied field values which appear too small to initiate the breakdown. In this paper we will show how an effective dielectric constant characterizing the dust layer can be determined from ac dielectric measurements and the theory of Debye. When combined with an expression for the enhanced local electric field in the void spaces between particles in the layer, field strengths which are large enough to initiate electrical breakdown in the layer are predicted at relatively low values of applied field. The effect of temperature and dust layer thickness on the onset of electrical breakdown within the dust layer can also be explained by the dependence of the effective dielectric constant on these parameters.

When a sinusoidal voltage is applied to a dielectric material, a leakage current will be induced within the dielectric in addition to the resulting charging current. The existence of both the leakage and charging currents is conventionally represented by the use of a complex dielectric constant

$$\epsilon^* = \epsilon' - i\epsilon'' \quad (1)$$

to describe the dielectric. Here, both ϵ' and ϵ'' are functions of frequency. The real part of the dielectric constant, ϵ' , is related to the equivalent parallel capacitance, C_p , of the material by

$$C_p = \epsilon' C_0 \quad (2)$$

where C_0 is the geometrical (air) capacitance of the measuring electrodes separated by a distance equivalent to the thickness of the dielectric. The imaginary part of the dielectric constant ϵ'' , is related to C_0 and the conductance, G , of the material according to

$$\epsilon'' = \frac{G(\omega)}{\omega C_0} \quad (3)$$

where ω is the angular frequency. By measuring C_p and G , ϵ' and ϵ'' can be determined from Equations 2 and 3, respectively.

If the dielectric material is sufficiently dipolar in nature, the theory of Debye¹ can be applied to ϵ^* :

$$\epsilon^* = \epsilon_\infty + (\epsilon_{dc} - \epsilon_\infty)/(1 + i\omega\tau_0) \quad (4)$$

where ϵ_∞ and ϵ_{dc} are the dielectric constants in the high and low frequency

limits, respectively; and τ_0 is the characteristic relaxation time. Equation 4 can be separated into its real and imaginary parts:

$$\epsilon'(\omega) = \epsilon_\infty + \frac{\epsilon_{dc} - \epsilon_\infty}{1 + (\omega\tau_0)^2} \quad (5)$$

$$\epsilon''(\omega) = \frac{\omega\tau_0(\epsilon_{dc} - \epsilon_\infty)}{1 + (\omega\tau_0)^2} \quad (6)$$

Cole and Cole² have shown that the Argand diagram of Equation 4 is a circular arc from which ϵ_{dc} can be extrapolated.

When the data for ϵ' and ϵ'' are somewhat scattered, Cole³ has shown that more useful forms of Equations 5 and 6 are obtained by multiplying both sides of each equation by $(1 + i\omega\tau_0)$ and solving for ϵ' in terms of ϵ'' and ϵ_{dc} :

$$\epsilon'(\omega) = \epsilon_{dc} - \tau_0(\omega\epsilon'') \quad (7)$$

For the purpose of extrapolating to ϵ_{dc} , Equation 7 has the advantage of being a linear equation with intercept ϵ_{dc} and slope $-\tau_0$.

Auty and Cole⁴ have shown that the contribution to ϵ'' from the dc conductance of the layer must be removed from Equation 3 before using Equation 7. This can be done by subtracting the dc conductance, G_{dc} , from the conductance at higher frequencies:

$$\epsilon''(\omega) = \frac{G(\omega) - G_{dc}}{\omega C_0} \quad (8)$$

where $G(\omega)$ is the conductance obtained from the measured parallel resistance of the sample.

Because of the particulate nature of a dust layer, its dielectric constant will vary with position in the material. However, when Debye's theory can be applied to the layer, an average, "effective" dielectric constant (ϵ_{dc}) can be ascribed to the dust layer.

Materials and Methods

The same test cell described in Part I of this study was connected to a digital RLC bridge (GenRad model 1689) and placed in an environmental chamber. For each temperature and test frequency, the measuring circuit was zeroed for its open- and short-circuit impedance to obtain accurate values for the dust layer impedance. Then the equivalent parallel capacitance and resistance were measured for several different frequencies between 12 Hz and 100 kHz at an applied voltage of 1 V rms. Varying the applied voltage throughout the range of the bridge (5 mV to 1.275 V) had no effect on the capacitance and conductance values which were measured. For measurement temperatures above 250°C, a standard resistivity cell (IEEE Standard 548-1984) was used. The transition from measurements made with one cell to those of the other cell was smooth. Thus, it was concluded that no offset or error was introduced into the measurements by changing test cells.

The technique of using bridge measurements to obtain the complex dielectric constant of a coal fly ash has been previously demonstrated by Tassicker⁵ and by Evans.⁶ Eleven different fly ash species were examined here. Since generally similar qualitative features were observed for these samples, the discussion will focus on the pulverized coal fly ash from the Wabamun Power Plant in Canada. The fly ash particles were predominantly spherical in shape and amorphous, with a mass median diameter of 33.5 μ m.

Results

The variation of ϵ' with frequency for the fly ash at 266°C and 9 percent wa-

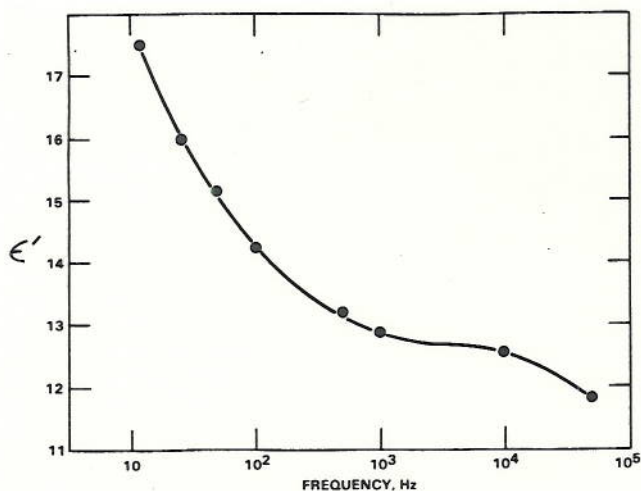


Figure 1. Real part of the dielectric constant of Wabamun fly ash at 266°C and 9 percent water vapor.

ter vapor (by volume) in the test environment is shown in Figure 1. The corresponding data for ϵ'' are shown in Figure 2. Here the value of G_{dc} in Equation 8 has been approximated by the conductance at 12 Hz (the lower limit of the RLC bridge). As a result, the data of Figure 2 begin at 20 Hz rather than 12 Hz. Notice that the sudden decline in ϵ' for frequencies greater than 10 kHz is accompanied by a sudden increase in ϵ'' in these regions. This resonance behavior was predicted by Debye¹ and lends support to the validity of using Debye's analysis on fly ash. Figure 2 suggests that another resonance occurs in the low frequency limit which is not clearly resolved in Figure 1. These dielectric constant data are in qualitative agreement with the earlier work of Tassicker and Evans. However, the present data more clearly resolve the Debye resonances because the earlier works did not correct for the dc conductance in the imaginary part of the dielectric constant. The measured parameters of capacitance and conductance were also in general agreement with the work of McLean and Pohl;⁷

quantitative comparisons are not possible because of the wide variation of humidity and temperature in that work.

A plot of Equation 7 for the data of Figures 1 and 2 is shown in Figure 3.

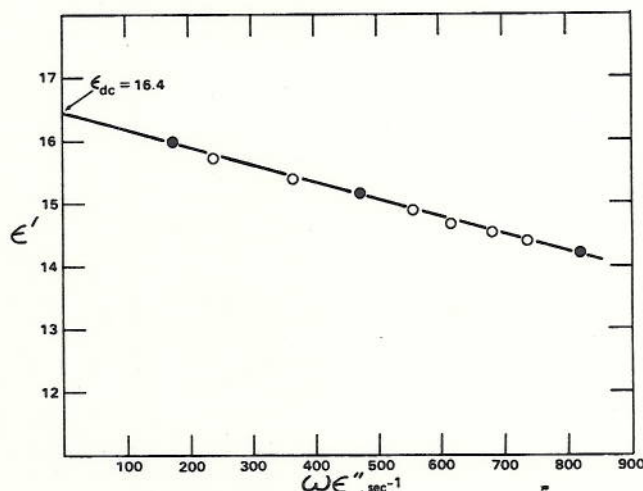


Figure 3. Plot of Equation 7 for Wabamun fly ash at 266°C and 9 percent water vapor.

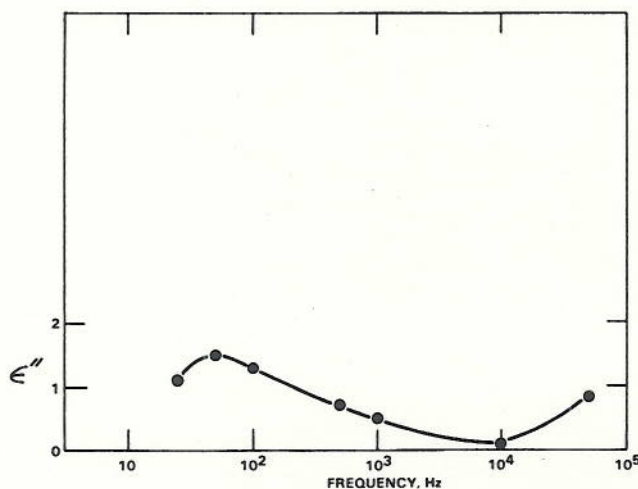


Figure 2. Imaginary part of the dielectric constant of Wabamun fly ash at 266°C and 9 percent water vapor.

Due to the broadness of the resonance in Figure 1 in the low-frequency region (indicating a distribution of relaxation times rather than a single τ_0), better correlation of the data results if the use of Equation 7 is restricted to measured (solid circles) and interpolated (open circles) values of ϵ' and ϵ'' in Figures 1 and 2 obtained at frequencies of 100 Hz or less. The interpolated values picked from the curves of Figures 1 and 2 are necessary because of the scarcity of data in this frequency range. Application of linear regression to the data in Figure 3 yielded a value of 16.4 for ϵ_{dc} with a correlation coefficient (r^2) of 0.99.

Applying the foregoing extrapolation procedure to data obtained at many different temperatures results in Figure 4. Generally, ϵ_{dc} is quite sensitive to temperature changes in the high temperature limit but becomes progressively less sensitive as the temperature decreases, approaching an asymptotic behavior in the low temperature limit. Also, the presence of moisture in the test atmosphere had little or no ef-

fect on the value of ϵ_{dc} obtained at a given temperature. Figure 5 shows the variation of ϵ_{dc} with dust layer thickness at three different temperatures. The relationship is essentially linear for the range of thicknesses used.

Discussion

It has been established in Part I of this work⁸ that electrical breakdown within a dust layer is an ordinary electron avalanche process originating in voids within the dust layer and obeying Paschen's Law. For the dust layers used in this study, Paschen's Law predicts electric field strengths at breakdown in the range of 235 to 365 kV/cm, depending on the temperature of the layer (see Part I⁸). Figure 6 shows the

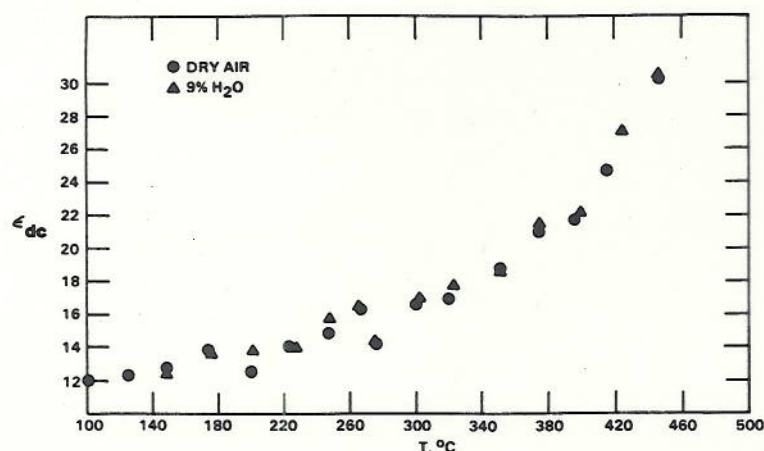


Figure 4. Variation of ϵ_{dc} with temperature of Wabamun fly ash.

dependence of the average electric field across the dust layer at breakdown, E_{BD} , on temperature for Wabamun fly ash in the presence of the indicated amounts of atmospheric moisture (volume percent). Since the average fields in this figure are in the range of 4 to 10 kV/cm, it is an enhanced local electric field in the void spaces between particles, E_{loc} , that corresponds to the breakdown field of Paschen's Law. McDonald, *et al.*,⁹ by treating the dust layer as a collection of spherical particles all of the same size and arranged in a cubic array, have shown that the combined effects of polarization and space charge due to a potential applied across the layer result in a maximum local electric field strength given by

$$E_{loc} \approx 1.5[1 + 1.25(\epsilon_{dc} - 1)]E_0 \quad (9)$$

where E_0 is the applied electric field. Using values of ϵ_{dc} of 12 and 31 at the temperature extremes of Figure 5, Equation 9 predicts local electric fields which are 22 to 58 times that of the applied field, in rough agreement with the predictions of Paschen's Law. Table I compares the values of E_{loc} obtained from Paschen's Law from the

Table I. Comparison of E_{loc} from Paschen's Law and from Equation 9.

Temperature (°C)	Figure 6 E_{BD} (kV/cm)	Figure 4 ϵ_{dc}	$E(9)$ (kV/cm)	$E(P)$ (kV/cm)	$\frac{E(P)}{E(9)}$
155	8	12.5	185	286	1.6
260	4	15.2	113	235	2.1

Table II. Correlation of ϵ_{dc} with E_{loc} from Equation 9 at 250°C.

Layer thickness (cm)	ϵ_{dc}	$E(9)$ (kV/cm)	$\frac{\epsilon_{dc}}{\epsilon_1}$	$\frac{E_1}{E(9)}$	% Difference of ratios
0.1	7.8	249	—	—	—
0.2	10.1	223	1.29	1.12	13
0.4	13.3	160	1.71	1.56	9
0.5	14.8	137	1.90	1.82	4
0.95	21.9	108	2.81	2.31	18

data of Earhart,¹⁰ $E(P)$, and those obtained using Figure 6 (9% H_2O) and Equation 9, $E(9)$. The two values agree within a factor of about two, which is remarkable considering the uncertainties and approximations involved in this comparison.

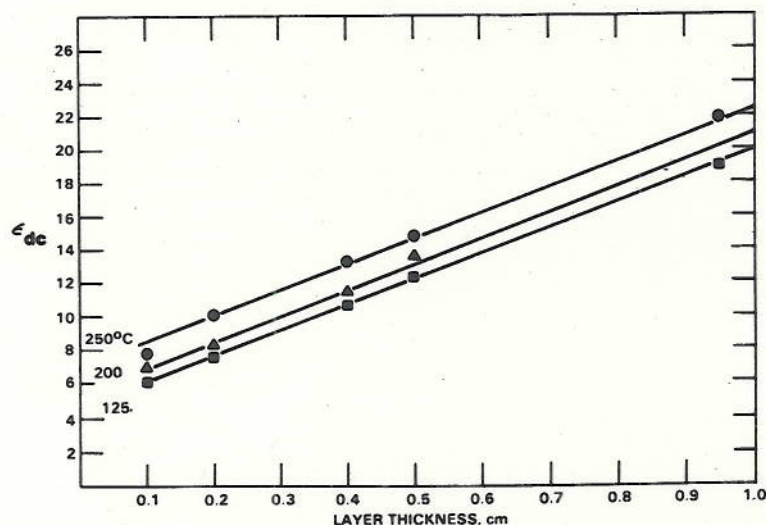


Figure 5. Variation of ϵ_{dc} with layer thickness of Wabamun fly ash.

The dependence of ϵ_{dc} on sample temperature has been shown by many investigators, including Debye.¹ A review of the important early work in this area was given by Fröhlich.¹¹ For temperatures above about 200°C, ϵ_{dc} increases rapidly with increasing temperature (Figure 4). Then Equation 9 predicts that progressively lower values of E_0 (E_{BD}) will be required to produce an E_{loc} of sufficient magnitude to initiate breakdown as the temperature increases. This agrees with the temperature dependence of the data of Figure 6 for a given humidity level. For lower temperatures, ϵ_{dc} becomes nearly independent of temperature and E_{BD} remains relatively constant as tem-

perature decreases. It has been shown in Part I of this work³ that the presence of moisture reduces the magnitude of E_{BD} necessary to initiate breakdown. However, the fact that ϵ_{dc} is not sensitive to the presence of moisture (Figure 4) indicates that the reduction in E_{BD} due to moisture is not connected with a change in ϵ_{dc} . Indeed, McLean and Pohl⁷ concluded that the effect of moisture (and temperature) is to change the dust layer's conductance, rather than causing any changes in the dielectric properties of the particles.

The details of the steady state charge exchange mechanism are not known. In any case, since the charge carriers within the dust layer are ionic,^{12,13} the metal electrode in the test cell is incapable of directly exchanging charge carriers with the layer surface. When an electric field is applied, the ionic charge carriers begin to migrate and this "blocking electrode" causes charge to build up just inside the dust layer at the electrode-layer interface. This layer of charges and the corresponding induced charges on the metal electrode constitute a "double layer" of charge at the

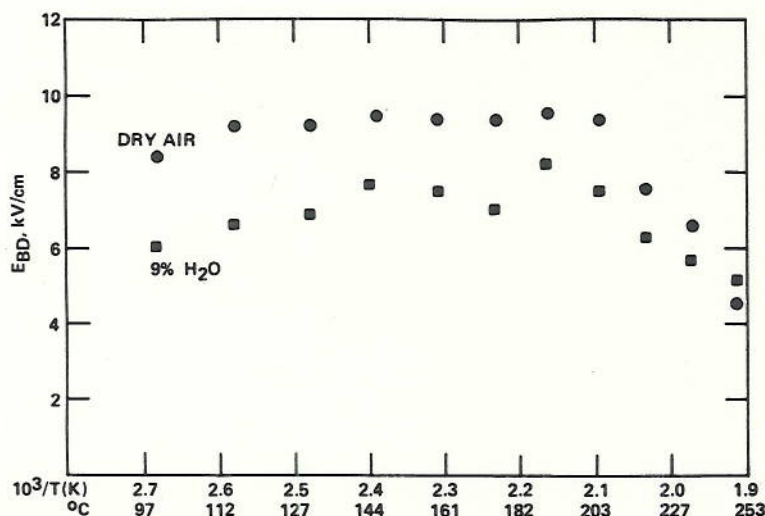


Figure 6. Variation of E_{BD} with temperature and moisture of Wabamun fly ash.

interface. A detailed analysis concerning the nature of this double layer is contained in the work of Conway.¹⁴ For our purpose, it is sufficient to note that the existence of the double layer at each electrode makes the test cell arrangement functionally equivalent to three capacitors in series. Then assigning an effective dielectric constant to the entire dust layer is tantamount to replacing the three capacitors by a single equivalent capacitor, using the usual reciprocal relationship for combining capacitors in series:

$$\frac{\epsilon_{dc}}{d} = \frac{\epsilon_1}{d_1} + \frac{\epsilon_2}{d_2} + \frac{\epsilon_3}{d_3} \quad (10)$$

where d is the total layer thickness; subscripts 1 and 3 refer to the capacitors formed by the double layers at each electrode; and subscript 2 refers to the capacitor formed by the intervening dielectric. Solving for ϵ_{dc} gives

$$\epsilon_{dc} = d \left[\frac{\epsilon_1}{d_1} + \frac{\epsilon_2}{d_2} + \frac{\epsilon_3}{d_3} \right] \quad (11)$$

Since the extent of the double layer is on the order of 1 nm,^{14,15} the first and third terms dominate the expression in the brackets since d_2 is on the order of a few millimeters. For simplicity, assume that $d_1 = d_3$ and $\epsilon_1 = \epsilon_3$. Then Equation 11 becomes

$$\epsilon_{dc} \approx \frac{2\epsilon_1}{d_1} d \quad (12)$$

But since $d \gg d_1$, region 2 in the dust layer would appear semi-infinite to region 1, so d_1 should be nearly constant and independent of d . Also, ϵ_1 should be constant for a given temperature. Then the dependence of ϵ_{dc} on layer thickness would be essentially linear, as the data of Figure 5 show.

Figure 7 shows the dependence of E_{BD} on dust layer thickness for the fly ash. In general, E_{BD} decreases as the thickness increases for a given tem-

perature. This behavior can now be readily explained by Equations 9 and 12 and the data of Figure 5: thicker dust layers have larger effective dielectric constants, so they require smaller values of E_{BD} to produce a given E_{loc} .

The data of Figures 5 and 7 can also be used to check the validity of the predictions of Equation 9. Table II shows the correlation between the ratios of ϵ_{dc} for 250°C to the ratios of E_{loc} from Equation 9, $E(9)$, normalized to the data for a 0.1 cm thickness (ϵ_1 and E_1). The agreement is quite good considering the roughness of the compari-

son. Thus, the technique used by McDonald *et al.* of combining the contributions of polarization and space charge within the layer appears to be justified.

Conclusions

Using ac dielectric measurements of dust layers and applying the theory of Debye allows the determination of an effective dielectric constant to characterize the layer. Combining this constant with an expression for the enhanced local electric fields across the voids between particles in the bulk where electrical breakdown occurs produces agreement with values of electrical field at breakdown predicted by Paschen's Law. The effective dielectric constant increases with increasing temperature and explains the corresponding decrease in applied electric field necessary to produce breakdown. For increasing dust layer thickness, the effective dielectric constant also increases, accompanied by a decrease in the applied field which will initiate breakdown.

Acknowledgment

This work has been sponsored by the Air and Energy Engineering Research Laboratory of EPA (Cooperative Agreements CR-808973 and CR-810284).

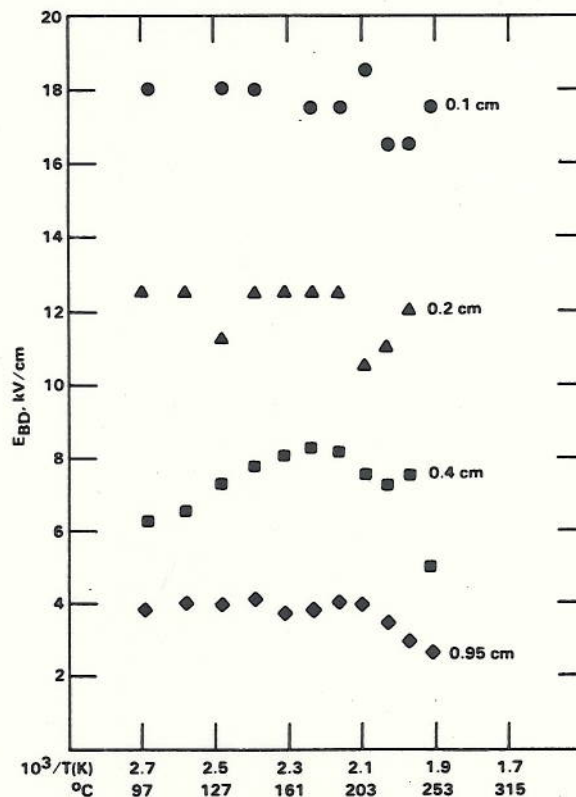


Figure 7. Variation of E_{BD} with layer thickness of Wabamun fly ash at 9 percent water vapor.

References

1. P. Debye, *Polar Molecules*, Chemical Catalog Co., New York, 1929.
2. K. S. Cole, R. H. Cole, "Dispersion and adsorption in dielectrics. I. Alternating current characteristics," *J. Chem. Phys.* 9: 341 (1941).
3. R. H. Cole, "On the analysis of dielectric relaxation measurements," *J. Chem. Phys.* 23: 493 (1955).
4. R. P. Auty, R. H. Cole, "Dielectric properties of ice and solid D₂O," *J. Chem. Phys.* 20: 1309 (1952).
5. O. J. Tassicker, "The temperature and frequency dependence of the dielectric constant of power-station flyash," *Staub-Reinhalt. Luft* 31: 23 (1971).
6. R. N. Evans, *The Dielectric Properties of Fly Ash from Western Coals*, Thesis, U. of North Dakota, 1978.
7. K. J. McLean, H. K. Pohl, "Dielectric properties and equivalent circuit of a high resistivity particulate layer," *J. Electrostatics* 8: 227 (1980).
8. R. P. Young, J. L. DuBard, L. E. Sparks, "The onset of electrical breakdown in dust layers: I. Microsparking described by Paschen's law," *JAPCA* 38: 1412 (1988).
9. J. R. McDonald, R. B. Mosley, L. E. Sparks, "An approach for describing electrical characteristics of precipitated dust layers," *JAPCA* 30: 372 (1980).
10. R. F. Earhart, "The discharge of electricity through gases at various temperatures," *Phys. Rev.* 31: 652 (1910).
11. H. Fröhlich, *Theory of Dielectrics*, Oxford University Press, London 1949, pp. 15-61.
12. R. E. Bickelhaupt, "Surface resistivity and the chemical composition of fly ash," *JAPCA* 25: 148 (1975).
13. R. E. Bickelhaupt, "Electrical volume conduction in fly ash," *JAPCA* 24: 251 (1974).
14. B. E. Conway, *Theory and Principles of Electrode Processes*, The Ronald Press Company, New York, 1965, pp. 25-43.
15. J. O. Bockris, A. K. N. Reddy, *Modern Electrochemistry*, Vol. 2, Plenum Press, New York, 1970, pp. 623-841.

Dr. Young is a research physicist and Dr. DuBard is head of the Applied Technology Division of the Environmental Sciences Department at Southern Research Institute, P.O. Box 55305, Birmingham, AL 35255-5305. Dr. Sparks is a project officer at the U.S. Environmental Protection Agency, Air and Energy Engineering Research Laboratory, Research Triangle Park, NC 27711. This paper was submitted for peer review May 2, 1986. The revised manuscript was received October 5, 1987.